Superresolved imaging in digital holography by superposition of tilted wavefronts

Vicente Mico, Zeev Zalevsky, Pascuala García-Martínez, and Javier García

A technique based on superresolution by digital holographic microscopic imaging is presented. We used a two dimensional (2-D) vertical-cavity self-emitting laser (VCSEL) array as spherical-wave illumination sources. The method is defined in terms of an incoherent superposition of tilted wavefronts. The tilted spherical wave originating from the 2-D VCSEL elements illuminates the target in transmission mode to obtain a hologram in a Mach–Zehnder interferometer configuration. Superresolved images of the input object above the common lens diffraction limit are generated by sequential recording of the individual holograms and numerical reconstruction of the image with the extended spatial frequency range. We have experimentally tested the approach for a microscope objective with an exact 2-D reconstruction image of the input object. The proposed approach has implementation advantages for applications in biological imaging or the microelectronic industry in which structured targets are being inspected.

OCIS codes: 090.0090, 100.6640, 110.0180.

1. Introduction

Digital holography can be used to reconstruct the phase information of objects and thus to improve the axial resolution of microscopy. Using digital holography techniques allows the hologram to be recorded with an electronic camera (normally a CCD camera) and the object wave to be reconstructed numerically.[1,2] Digital holography reconstruction simulates the optical beam propagation of the complex amplitude by discrete implementation of the Kirchhoff–Fresnel propagation equations. Various experimental setups extracting the three-dimensional (3-D) information and performing phase-contrast imaging and pattern recognition have been studied by using digital holography.[3–5] However, the main problem in digital holography is the resolution of the CCD devices, which is lower than photographic materials by at least an order of magnitude. To overcome this limitation, researchers have proposed phase-shifting digital holography that uses an in-line setup to decrease the fringe spacing and the phase shifting of the reference beam to evaluate directly the complex amplitude at the CCD plane and thus to eliminate the conjugate images completely.[6] Phase-shifting digital holography has also been applied to 3-D microscopy.[7] Moreover, a dramatic improvement can be achieved by use of synthetic apertures. The basic idea is to combine holograms recorded at different camera positions to construct a large digital hologram.[8,9] However, these methods use an expensive, high-precision mechanical movement and are time consuming.

In this paper we apply superresolution techniques by using digital holography tools. In fact, the ability to improve the limited resolving power of optical systems, which is due to the wave nature of light, has been widely studied in the past[10–14] for both theoretical and practical benefits. Generally, the numerical aperture (NA) determines the diffraction cutoff frequency of the system up to a maximum lateral resolution of $\lambda/2$ with a constant wavelength. An increase of the NA represents a resolution improvement. However, high-NA systems are complex and difficult to implement. Thus superresolution techniques have been proposed over the years to enlarge the aperture of the system without changing the physical properties of the NA for the lenses. Some of those techniques to improve the superresolution are based on studying the information capacity of the system,[10–12] which is a measure of the number of degrees of freedom for optical systems by means of an invariance theorem.

V. Mico is with AIDO, Technological Institute of Optics, Colour, and Imaging, C/. Nicolás Copérnico, 7-13 Parc Tecnològic, 46980 Paterna (Valencia), Spain. Z. Zalevsky is with the School of Engineering, Bar-Ilan University, Ramat-Gan 52900, Israel. P. García-Martínez and J. García (javier.garcia.monreal@uv.es) are with Departmento de Optica, Universitat de Valencia, C/. Dr. Moliner 50, 46100 Burjassot, Spain.

Received 18 May 2005; revised 23 August 2005; accepted 24 August 2005.

0003-6935/06/050822-07$15.00/0

The theorem from Refs. 10 and 11 states that it is not the spatial bandwidth but the information capacity of an imaging system that is constant. Then it is possible to extend the spatial bandwidth by encoding–decoding the additional information onto the unused parameters of the imaging system.[10,13] Bearing this fundamental principle in mind, we note that one of the most appealing approaches for achieving resolving power is related to temporally restricted objects, and it is based on two moving gratings.[13,14] The main idea is to introduce optical elements, such as gratings, that will divert the higher spatial frequency components into the aperture of the optical imaging system.

Recently, some authors used an interferometric approach to improve the optical resolution of an optical system. Thus Chen and Brueck[15] and Schwarz *et al.*[16] used off-axis illumination to change the high-frequency components generated when the illumination beam impinges the object into low-frequency components in such a way that these components can pass through the aperture of the system. By means of an interferometric register, these transmitted object spectrum components are shifted back toward their original location. Then the individual recorded intensities are added incoherently. The same effect of incoherent addition can be obtained by using mutually incoherent light sources for recording all the spatial frequency bands in a single step. Bearing this idea in mind, Mico *et al.*[17] used a one-dimensional (1-D) vertical-cavity self-emitting laser (VCSEL) array to illuminate an imaging system with a limited aperture. The holographic recording process was accomplished by interfering the spatial frequencies of the object with multiple complementary reference plane waves coming from the Mach–Zehnder interferometer. Contrary to Refs. 15 and 16, the transmission of all the spatial frequencies occurs at the same instant, using the spatial multiplexing of all the incoherent illumination sources. Moreover, the complexity of the system is not penalized by the inclusion of additional frequency slots, and more than three frequency bands can be added in the final image. In fact, the authors have used five sources simultaneously (for a fivefold increase of the system's spatial frequency bandwidth) as compared with the three illumination angles for the system presented in Ref. 17.

Although Leith *et al.*[18] and Sun and Leith[19] used incoherent sources to increase the resolution of imaging systems, such incoherent illumination has the disadvantage of reducing the dynamic range of the CCD and of increasing the cross talk between the recorded images. The combination of a similar coding approach together with a VCSEL line array was studied for the first time in Ref. 17. One of the main advantages of this system is that the coherence length between neighboring emitters is very short (close to the optical wavelength), which means that the variations of the temporal phase are made at the speed of light instead of at the much larger coherent lengths obtained by using diffusers. Moreover, high optical intensity was achieved in the VCSEL array (up to 10 mW). Another advantage of the system presented in Ref. 17 is that the VCSELs can be temporally modulated up to several gigahertz. Note that the 2-D VCSEL array is transversally incoherent (the sources are spatially incoherent to each other). The superresolving approach allows transmission of higher spatial frequencies, meaning that it generates a synthetic aperture that is wider than the true aperture of the imaging lens. As will be proved in the mathematical derivation in Section 2, the synthetic aperture generated by the suggested approach is actually a convolution operation between the VCSEL line array and the coherent transfer function (CTF) of the system. By temporally varying the relative amplitudes of each line array source, one can synthesize any synthetic transfer function. Thus an ultrafast (at a gigahertz rate) tunable spatial filter may be generated. In spite of all its previously demonstrated advantages, the system was difficult to align and the superresolution was obtained for only one direction.

Presented in this paper is a generalization of the approach shown in Ref. 17 that is applied to microscopic imaging and expanded into 2-D. As a main improvement, the illumination of the system is performed by using spherical tilted waves coming from a 2-D VCSEL array. In this way we significantly reduce the implementation complexity of the former system. Once the hologram is obtained, we perform the reconstruction digitally by use of a divergent reference beam or by addition of a quadratic phase function. Significant improvement in the resolution of a commercial microscope objective with NA = 0.1 and 5× magnification is demonstrated.

2. Theoretical Analysis of the Optical System

The optical setup is shown in Fig. 1. A Mach–Zehnder interferometric configuration is used to implement the technique. The 2-D VCSEL array illuminates the interferometric system.

The first beam splitter (BS1) is used to distribute the incoming light to two optical beam paths. In the first optical path (the imaging arm) the object is illuminated by a spherical wave and imaged by the microscope objective into the CCD after reflection in a mirror (M2). In the other optical path (the reference arm) the light is directed toward the CCD using a mirror (M1). A second beam splitter (BS2) mixes the two beams into the image plane and produces the holographic register. By tilting the beam splitter BS1 and the mirror M1 accordingly, we produced tilting of the reference beam versus the imaging beam of the interference pattern. It is well known that a low-pass version of the input object is obtained in the image plane when the light comes from the imaging arm and on-axis illumination is used. In this paper we will improve the resulting imaging resolution of the input object by taking the influence of many VCSEL sources that illuminate the interferometric system.

A hologram of a microscopic object is recorded by an image sensor (CCD), and numerical reconstruction is performed by a computer, using standard Fourier-transform techniques. In this section we review the

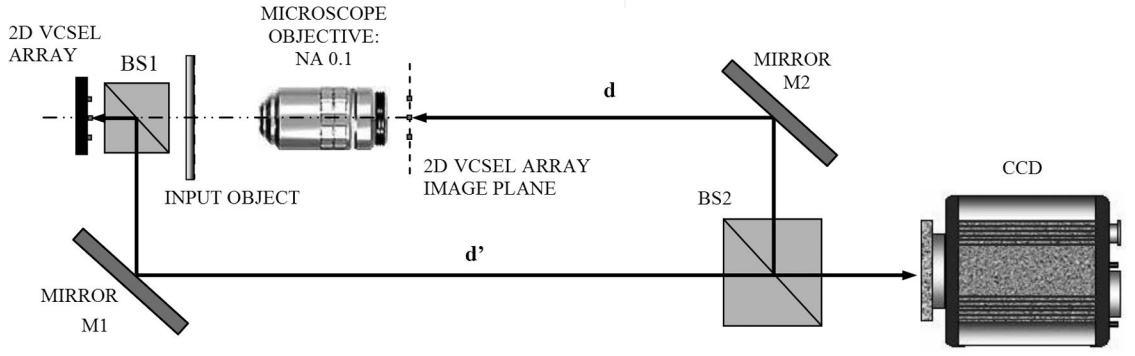

Fig. 1. Experimental setup. The object is imaged onto the CCD by the microscope lens. Divergence distances for the illumination in both arms, d and d', are indicated by the broken segments ending with arrows.

mathematical foundations of diffraction analysis. We define the input's wavefront $f(x, y)$ and the Fourier transform of the object's wavefront as $\tilde{f}(u, v)$, where (x, y) and (u, v) are the spatial and spatial frequency coordinates, respectively.

In this paper we employ a 2-D $m \times n$ source array in which every element emits spherical waves to illuminate the input object. Then the amplitude distribution onto the CCD by the imaging arm for each VCSEL source (with indices m and n) with spherical illumination and under quadratic approximation is

$$U_{m,n}^{\mathrm{CCD}}(x, y) = \left(f\left(-\frac{x}{M}, -\frac{y}{M}\right) \exp\left\{ j \frac{k}{2Md} [(x - x_m)^2 + (y - y_n)^2] \right\} \right) \otimes \mathrm{disk}(\Delta v r), \tag{1}$$

where M is the imaging magnification, k is the wavenumber, d is the distance between the VCSEL array image plane through the microscope objective and the CCD, (x_m, y_n) are the coordinates of the off-axis VCSEL source, r is the polar coordinate defined as $r = (x^2 + y^2)^{1/2}$, and $\mathrm{disk}(\Delta v r)$ is the point-spread function (PSF) of the optical microscope lens.

From Fig. 1, the intensity distribution recorded at the CCD plane comes from the addition of Eq. (1) and a spherical reference beam as

$$I_{m\times n}^{\mathrm{CCD}}(x, y) = \left| \left(f\left(-\frac{x}{M}, -\frac{y}{M}\right) \exp\left\{ j \frac{k}{2Md} [(x - x_m)^2 + (y - y_n)^2] \right\} \right) \otimes \mathrm{disk}(\Delta v r) + \exp\left\{ j \frac{k}{2d'} [(x - x_m)^2 + (y - y_n)^2] + j 2\pi Q x \right\} \right|^2, \tag{2}$$

where d' is the distance from the 2-D VCSEL array to the CCD and Q is the carrier frequency introduced in the x axis. The last expression can be split into the four terms $P_1(x, y)$, $P_2(x, y)$, $P_3(x, y)$, and $P_4(x, y)$:

$$\begin{aligned} I_{m,n}^{\mathrm{CCD}}(x, y) = 1 &+ \left| \left(f\left(-\frac{x}{M}, -\frac{y}{M}\right) \exp\left\{ j \frac{k}{2Md} [(x - x_m)^2 + (y - y_n)^2] \right\} \right) \otimes \mathrm{disk}(\Delta v r) \right|^2 \\ &+ \left[\left(f\left(-\frac{x}{M}, -\frac{y}{M}\right) \exp\left\{ j \frac{k}{2Md} [(x - x_m)^2 + (y - y_n)^2] \right\} \right) \otimes \mathrm{disk}(\Delta v r) \right] \exp\left\{ -j \frac{k}{2d'} \times [(x - x_m)^2 + (y - y_n)^2] - j 2\pi Q x \right\} \\ &+ \left[\left(f^*\left(-\frac{x}{M}, -\frac{y}{M}\right) \exp\left\{ -j \frac{k}{2Md} \times [(x - x_m)^2 + (y - y_n)^2] \right\} \right) \otimes \mathrm{disk}(\Delta v r) \right] \\ &\times \exp\left\{ j \frac{k}{2d'} [(x - x_m)^2 + (y - y_n)^2] + j 2\pi Q x \right\}. \end{aligned} \tag{3}$$

Equation (3) represents the hologram registered in the CCD for a single VCSEL centered at (x_m, y_n). To obtain the reconstruction, we perform a digital inverse Fourier transformation and we analyze each term separately. The Fourier transform of the first term $[\tilde{P}_1(u, v)]$ is just a delta function centered at the origin. The Fourier transform of the second term $[\tilde{P}_2(u, v)]$, also centered at the origin, is the autocorrelation of the bandpass slot. The Fourier transform of the third term, $[\tilde{P}_3(u, v)]$, is a bandpass of the object spectrum placed at the left position of the central autocorrelation term (-1 diffraction order for the holographic recording process):

$$\tilde{P}_3(u,\ v) = K\Bigg\{\Bigg[\tilde{f}\Big(Mu + \frac{x_m}{\lambda d},\ Mv + \frac{y_n}{\lambda_d}\Big) \otimes \mathrm{FT}^{-1}\Big\{\exp\Big[j\,\frac{k}{2Md}\,(x^2 + y^2)\Big]\Big\}\Bigg]\mathrm{circ}\Big(\frac{\rho}{\Delta\nu}\Big)\Bigg\} \otimes \mathrm{FT}^{-1}\Big\{\exp\Big[-j\,\frac{k}{2d'}\,(x^2 + y^2)\Big] \times \exp\Big[j\,\frac{k}{d'}(xx_m + yy_n)\Big]\Big\} \otimes \delta(u + Q,\ v), \quad (4)$$

where $\tilde{P}_3(u, v)$ is the Fourier transform of the third term of Eq. (3) and K is a constant that includes constant phase factors. The first convolution of Eq. (4) would produce a defocus in the Fourier plane. Moreover, it is restricted to a limited extension in the frequency domain defined by the circ function. This means that the transmitted bandpass of the object spectrum is defocused inside the limited region, and because of that a corrected reconstruction cannot be obtained. To correct the reconstruction of the object, we need to digitally compensate for this defocusing effect by multiplying the recorded hologram by the conjugated spherical phase factor before Fourier transformation. This will eliminate the quadratic phase factors in Eq. (4). With this modification, Eq. (4) can be rewritten as

$$\tilde{P}_3(u,\ v) = K\Bigg\{\Big[\tilde{f}\Big(Mu + \frac{x_m}{\lambda d},\ \ Mv + \frac{y_n}{\lambda d}\Big)\Big]\mathrm{circ}\Big(\frac{\rho}{\Delta\nu}\Big)\Bigg\} \otimes \mathrm{FT}^{-1}\Big\{\exp\Big[j\,\frac{k}{d'}\,(xx_m + yy_n)\Big]\Big\} \otimes \delta(u + Q,\ v). \quad (5)$$

Equation (5) describes the information of the spectral frequency bandpass of the object spectrum transmitted by the pupil microscope objective. The linear phase factor moves the transmitted spectral bandpass from the central terms. However, to guarantee the separation between orders, we have also added a carrier frequency offset, which corresponds to a tilt of the reference plane.

Now, if we consider all the illumination sources from the 2-D VCSEL array, Eq. (6) can be rewritten as

$$\tilde{P}_3^{\mathrm{sum}}(u,\ v) = K\Bigg\{\sum_{m,n}\Big[\tilde{f}\Big(Mu + \frac{x_m}{\lambda d},\ \ Mv + \frac{y_n}{\lambda d}\Big) \times \mathrm{circ}\Big(\frac{\rho}{\Delta\nu}\Big)\Big] \otimes \delta\Big(u + \frac{x_m}{\lambda d'},\ \ v + \frac{y_n}{\lambda d'}\Big)\Bigg\} \otimes \delta(u + Q,\ v). \quad (6)$$

The term enclosed by square brackets represents the different frequency bands of the object selected by the circ function since, as seen in Eq. (6), this function multiplies the spectrum $\tilde{f}$. Moreover, from Eq. (6) the frequency bands are shifted according to the distance d' and the bias carrier frequency Q. In fact, what we are performing digitally is a synthetic aperture, as depicted in Fig. 2. It represents the desired configuration of the different frequency bands. Note that the frequency bands are centered at positions different from the displacements introduced by the delta functions. By properly adjusting the axial distances and the magnification, one could obtain all terms overlapping at the desired locations. Nevertheless, to further simplify the setup, we used five VCSEL sources arranged in a cross shape and lighted them sequentially. The sequential illumination permits us to register different frequency bands of the object separately, without having to take care of the matching between scaling and displacement of the bands. The arrangement of the frequency bands is performed digitally at a later stage.

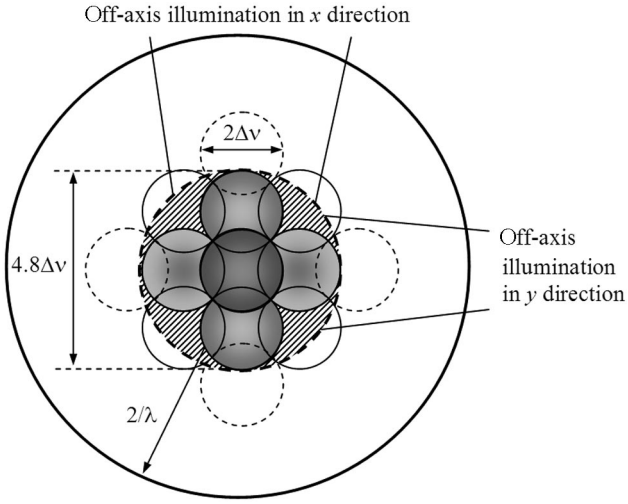

Fig. 2. Synthetic aperture generation.

The size of the smallest circles in Fig. 2 corresponds to the NA of the microscope objective ($\Delta\nu$ radius). We selected circular frequency bandpasses so that when they are located at their proper positions, the center-to-center spacing is $\Delta\nu/\sqrt{2}$, allowing full coverage of the frequency plane. The synthetic pupil (dashed circle of $\sim 4.8\Delta\nu$ diameter) is generated by two off-axis illuminations in each perpendicular direction, expanding the actual cutoff frequency to nearly five times the conventional frequency cutoff. Once we capture the hologram, we can digitally separate the multiplexed frequency bands. After digital postprocessing, we obtain the spectrum according to Fig. 2. An inverse Fourier transform recovers the superresolved object. Owing to the high switching speed of the VCSELs and their high-energy throughput, provided that no adjustment is needed, the full sequence can be captured at a fast rate. Moreover, the digital processing is not time consuming, as it involves only linear and simple calculations. Nevertheless, it would be possible to capture all the spectral bands in one shot, in a manner similar to that reported in Ref. 17. One would only need to add an additional imaging optical system in the reference arm.

Notice that no assumption is made about the prop-

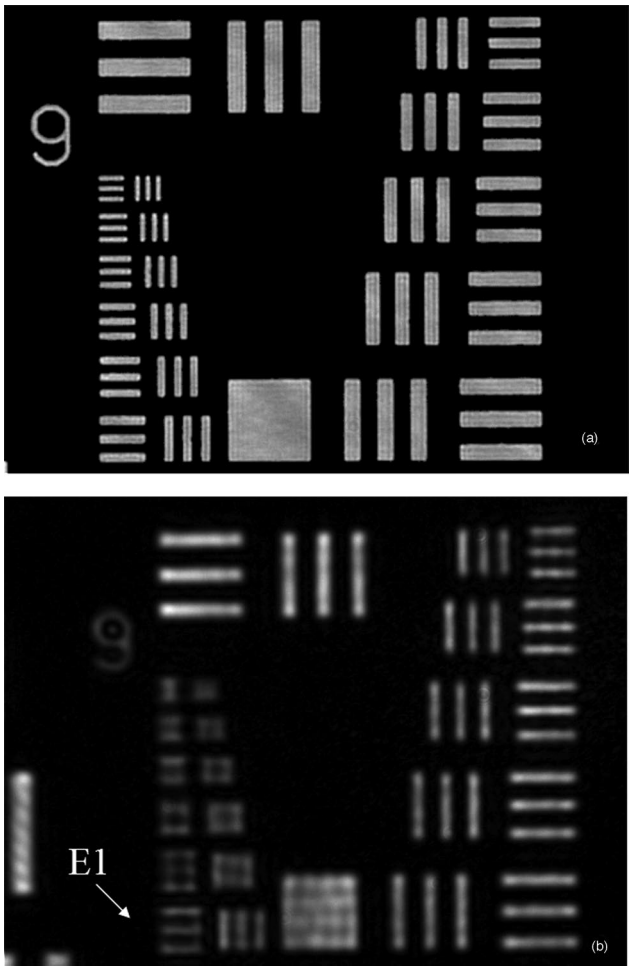

Fig. 3. (a) Reference high-resolution image obtained with a 0.42 NA microscope lens and incoherent illumination. (b) Image obtained with a 0.1 NA microscope lens and single-VCSEL (coherent) illumination.

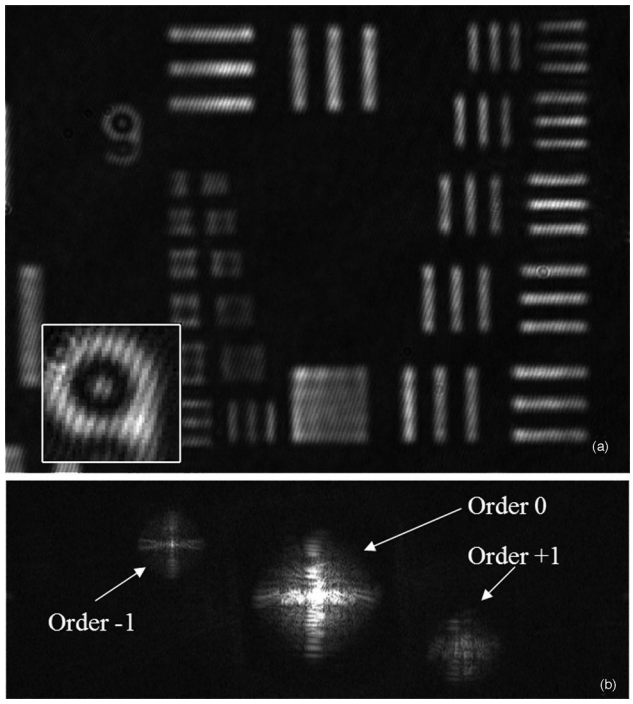

Fig. 4. (a) Hologram image obtained by illumination with the central VCSEL. The inset shows a magnified portion of the image, in which the fringes can be observed. (b) Image in the corresponding virtual Fourier-transform plane of (a) that underwent a previous multiplication by a spherical phase factor to focus the −1 order.

erties of the object $f(x, y)$, so for any complex input distribution we will always reconstruct the input. Also, there is no need to adjust the spherical-wave curvature between the two interferometric arms. As a result, the system gains in simplicity and versatility. Contrary to Refs. 15 and 16, our system has no pupil filter in the system's Fourier plane (Ref. 15), and there is no need to change the implementation to add the different frequency bandpass of the object to the final image (Ref. 16).

3. Experimental Results

We tested the proposed superresolution method experimentally in a system as shown in Fig. 1. We use a Nikon microscope objective with a NA of 0.1 and a 5× magnification. Note that a large working distance, as needed in many practical applications, is usually related to a low NA. For the optical experiments, an array of 3 × 3 VCSELs are used. The input object is a U.S. Air Force resolution test. The sources are transverse single mode and monochromatic with $\lambda = 850$ nm. The objective, as given by its NA, has a resolution spot size of 4.25 μm. To compare the results obtained with our system, we show in Fig. 3(a) a high-resolution image of the test object by using a Mitutoyo microscope objective with a NA of 0.42 and incoherent illumination (cutoff frequency of 2000 line pairs/mm). In Fig. 3(b) the optical image obtained using illumination by a single VCSEL with the 0.1 NA lens is shown. Clearly, many spatial frequencies are not transferred by the low-NA objective, and a low-pass version of the test is obtained. Note that, in comparison with the previous incoherent image, aside from the much lower resolution, the coherent noise has appeared, spoiling the signal-to-noise ratio (SNR) of the image. The smallest resolved detail is ~4 μm, corresponding to element 1 (E1) in group 7 of the test, shown in Fig. 3(b).

As an example of the holograms captured in the CCD of the system, Fig. 4(a) shows the image corresponding to illumination by the central source. Figure 4(b) displays the Fourier transform of the digitally recorded hologram. A spherical phase factor [see Eq. (4)] was multiplied by the hologram to focus the −1 order [at the left in Fig. 4(b)] containing the bandpass. The zero order and the +1 order are focused improperly as a consequence. Note that the carrier frequency has shifted from zero (tilting the reference mirror) for separating the spatial frequency slot from the zero-order terms.

The different holograms, that correspond to different spatial frequency slots are taken in sequence and

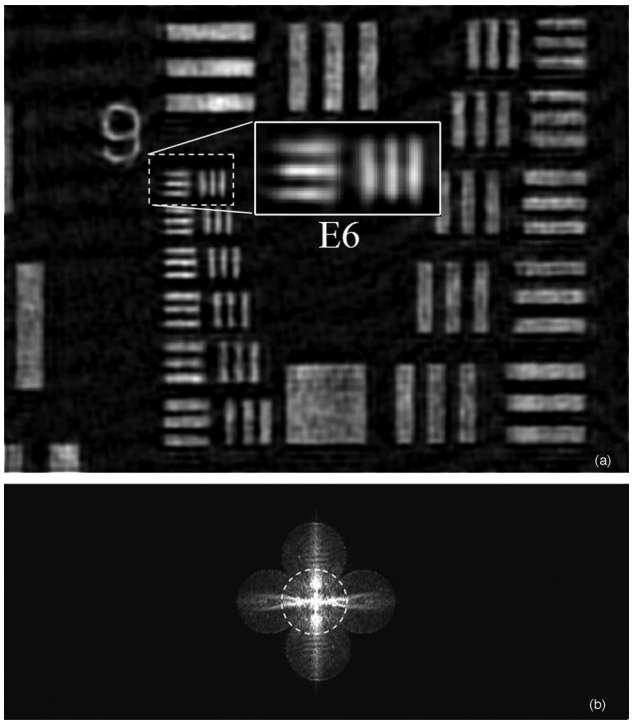

Fig. 5. (a) Image obtained with the 0.1 NA lens and the superresolution approach. (b) Fourier transform of (a) showing the extended synthetic aperture. The dashed circle shows the original aperture.

stored in the computer memory. Then the regions of interest (order -1) of each one are shifted to their proper spectral positions and superimposed to synthesize the synthetic aperture. An inverse Fourier transform yields the final superresolved image. Figure 5(a) shows the reconstructed image. Owing to 2-D VCSEL off-axis illumination, both vertical and horizontal resolution will be improved. It is obvious to see the gain in resolution with respect to the image in Fig. 3(b). According to theory, the resolution has been enhanced by a factor of 2.4 in both the horizontal and the vertical directions, giving a resolution spot size of 1.8 μm, which is sufficient to resolve the smallest details in the target [2.2 μm details corresponding to element 6 (E6) of group 7 in the test pattern]. Comparing the minimum resolvable detail size without the superresolving approach (4 μm) with the resolution obtained with our method (2.2 μm) demonstrates an enhancement of nearly a factor of 2 in the resolution. The test object has almost no oblique frequencies in the spectrum, so there is no need to add the diagonal frequency bands (those areas that appear dashed in Fig. 2). We note the lower SNR of the image as compared with the coherent image or even with the low-pass image. The most visible noise is the striped background on the image, covering what should be black regions. In fact, these areas have a low, although not null, transparency. Thus a low-bias amplitude will be registered in the holograms and will contribute to the output. In an incoherent system this bias will just cause a uniform background that can be eliminated from the image simply by subtracting a constant. In the case of an image made by multiple bandpasses, all the biases will interfere. Ideally, the addition would be uniform and would provide a uniform background. In practice, small misalignments between the beams will result in a low-contrast interference pattern that has spatial variations.

Finally, Fig. 5(b) depicts the Fourier transform of the reconstructed superresolved image. The bandpass due to the central VCSEL, which is coincident with the one shown in Fig. 4(b), is highlighted by a dashed circle. The added bandpasses are clearly visible, aside from the gain in lateral resolution.

4. Conclusions

In this paper a digital holographic technique to improve superresolution based on a 2-D array of mutually incoherent VCSELs sources has been presented. The principle is based on multiple superposition of digital image holograms performed by using different spherical tilted-wave illumination. The spatial frequency bands are sequentially transmitted through the lens owing to different positions of the illumination sources, and this information is recorded by using an interferometric configuration. Finally, a hologram is recorded and the reconstruction is obtained digitally by adjusting the focusing process numerically for each frequency band. After focusing, the superresolved object is reconstructed by Fourier transformation. The main advantages of our method are the possibility of recording all the interferograms without changing the setup and its simplicity. Since the VCSEL array can be modulated in rates of a few gigahertz, the hologram recording is performed temporally almost at once. Moreover, no assumption is made about the object, so the method can be used for more complicated objects, including phase objects. This is the main difference between this study and others of incoherent illuminated holographic recording.

This research was supported by Fondo Europeo de Desarrollo Regional funds and the Spanish Ministerio de Educación y Ciencia under project FIS2004-06947-C02-01, the Direcció General d'Investigació i Transferència Tecnològica under project IIARC0/2004/217, and the Agencia Valenciana de Ciencia y Tecnología (AVCT) under project GRUPOS03/117.

References

1. W. S. Haddad, D. Cullen, J. C. Solem, J. W. Longworth, A. McPherson, K. Boyer, and C. K. Rhodes, "Fourier-transform holographic microscope," Appl. Opt. **31,** 4973–4978 (1992).
2. U. Schnars and W. P. O. Jüpter, "Direct recording of holograms by a CCD target and numerical reconstruction," Appl. Opt. **33,** 179–181 (1994).
3. B. Nilsson and T. E. Carlsson, "Direct three-dimensional shape measurement by digital light-in-flight holography," Appl. Opt. **37,** 7954–7959 (1998).
4. E. Cuche, F. Bevilacqua, and C. Depeursinge, "Digital holography for quantitative phase contrast imaging," Opt. Lett. **24,** 291–293 (1999).
5. F. Dubois, C. Minetti, O. Monnom, C. Yourassowsky, and J.-C. Legros, "Pattern recognition with digital holographic micro-

scope working in partially coherent illumination," Appl. Opt. **41,** 4108–4119 (2002).
6. I. Yamaguchi and T. Zhang, "Phase-shifting digital holography," Opt. Lett. **22,** 1268–1270 (1997).
7. I. Yamaguchi, J.-I. Kato, S. Otha, and J. Mizuno, "Image formation in phase-shifting digital holography and applications to microscopy," Appl. Opt. **40,** 6177–6186 (2001).
8. F. Le Clerc, M. Gross, and L. Collot, "Synthetic aperture experiment in the visible with on-axis digital heterodyne holography," Opt. Lett. **26,** 1550–1552 (2001).
9. J. H. Massig, "Digital off-axis holography with a synthetic aperture," Opt. Lett. **27,** 2179–2181 (2002).
10. G. Toraldo di Francia, "Resolving power and information," J. Opt. Soc. Am. **45,** 497–501 (1955).
11. G. Toraldo di Francia, "Degrees of freedom of an image," J. Opt. Soc. Am. **59,** 799–804 (1969).
12. I. J. Cox and J. R. Sheppard, "Information capacity and resolution in an optical system," J. Opt. Soc. Am. A **3,** 1152–1158 (1986).
13. W. Lukosz, "Optical systems with resolving powers exceeding the classical limits. II," J. Opt. Soc. Am. **57,** 932–941 (1967).
14. A. Shemer, D. Mendlovic, Z. Zalevsky, J. Garcia, and P. Garcia-Martinez, "Superresolving optical system with time multiplexing and computer decoding," Appl. Opt. **38,** 7245–7251 (1999).
15. X. Chen and S. R. J. Brueck, "Imaging interferometric lithography: approaching the resolution limits of optics," Opt. Lett. **24,** 124–126 (1999).
16. C. J. Schwarz, Y. Kuznetsova, and S. R. J. Brueck, "Imaging interferometric microscopy," Opt. Lett. **28,** 1424–1426 (2003).
17. V. Mico, Z. Zalevsky, P. Garcia-Martinez, and J. Garcia, "Single step superresolution by interferometric imaging," Opt. Express **12,** 2589–2596 (2004).
18. E. N. Leith, D. Angell, and C.-P. Kuei, "Superresolution by incoherent-to-coherent convergence," J. Opt. Soc. Am. A **4,** 1050–1054 (1987).
19. P. C. Sun and E. N. Leith, "Superresolution by spatial-temporal encoding methods," Appl. Opt. **31,** 4857–4862 (1992).